

## Mechanical, Dielectric, and Electromechanical Properties of Silicone Dielectric Elastomer Actuators

Il Jin Kim,<sup>1,2</sup> Kyoungho Min,<sup>1</sup> Hyunchul Park,<sup>1</sup> Soon Man Hong,<sup>1,3</sup> Woo Nyon Kim,<sup>2</sup> Seung Hyun Kang,<sup>4</sup> Chong Min Koo<sup>1,3</sup>

<sup>1</sup>Center for Materials Architecturing, Korea Institute of Science and Technology, Hwarangno 14-Gil 5, Seongbuk-Gu, Seoul 136-791, Republic of Korea

<sup>2</sup>Department of Chemical and Biological Engineering, Korea University, Sungbuk-Gu, Seoul 136-701, Republic of Korea

<sup>3</sup>Nanomaterials Science and Engineering, University of Science and Technology, 176 Gajung-Dong, 217 Gajungro Yuseong-Gu, Daejeon 305-350, Republic of Korea

<sup>4</sup>Central Research Institute Silicone Research Team, KCC Corporation, 83 Mabook-Dong, Giheung-Gu, Yongin-Si Gyunggi-Do, Republic of Korea

Correspondence to: C. M. Koo (E-mail: koo@kist.re.kr)

**ABSTRACT:** Silicone elastomer actuators were investigated to develop a simple and industrially scalable product with improved mechanical properties, such as a low modulus, high tearing strength, and good resilience, and enhanced electromechanical actuation properties. Silicone elastomers were fabricated via a hydrosilylation addition reaction with a vinyl-end-functionalized poly(dimethyl siloxane) (V), a multivinyl-functionalized silicone resin, and a crosslinker in the presence of a platinum catalyst. For the larger electromechanical actuation response, the silicone dielectric elastomer actuator had to have a larger molecular weight of poly(dimethyl siloxane), a smaller hardener content, and a resin-free composition. However, the silicone elastomer actuators needed to include a small amount of resin to improve the tearing strength. © 2013 Wiley Periodicals, Inc. *J. Appl. Polym. Sci.* 2014, 131, 40030.

**KEYWORDS:** crosslinking; dielectric properties; elastomers; sensors and actuators

Received 31 May 2013; accepted 2 October 2013

DOI: 10.1002/app.40030

### INTRODUCTION

The production of dielectric elastomer actuators (DEAs), devices for converting electrical to mechanical energy, have been a fast-growing and promising research field in recent years because of the outstanding advantages of DEAs, such as their large electromechanical strain, fast response, low cost, and facile processability.<sup>1–6</sup> They have been considered as good candidate materials for optical lenses, robotics, haptic displays, loudspeakers, active vibration damping, and muscle replacement.<sup>7–13</sup>

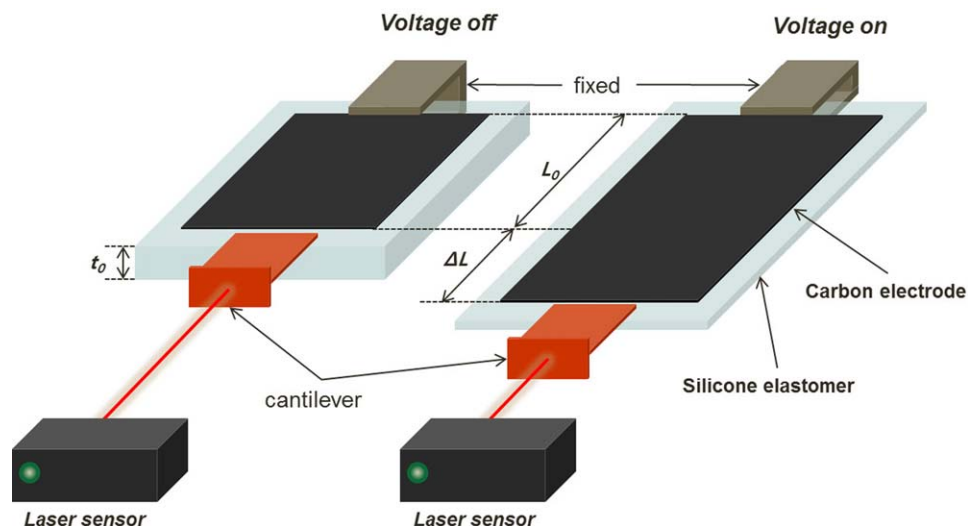
DEA is basically a compliant capacitor consisting of a deformable dielectric elastomer and compliant electrodes, as shown in Scheme 1. When an electric field is applied to the electrodes, the DEA is squeezed in the thickness direction and is expanded in area as a result of Maxwell stress, which originates from the Coulomb interaction between oppositely charged compliant electrodes.<sup>1,14</sup> The resulting electromechanical actuation strain ( $s$ ) is expressed by eq. (1):

$$S = \frac{1 - \epsilon_r \epsilon_0 E_f^2}{2E} \quad (1)$$

where  $\epsilon_0$  and  $\epsilon_r$  are the vacuum permittivity ( $8.85 \times 10^{-12}$  F/m) and the relative dielectric constant of the material, respectively, and  $E_f$  and  $E$  are the electric field (V/ $\mu\text{m}$ ) and modulus (MPa), respectively.

Dielectric elastomers usually consist of a polymer network and are capable of regaining their shape and size after deformation. The network is a three-dimensional entity of polymer chains connected with covalent bonds that are introduced through crosslinking reaction of a functional polymer with a crosslinker. Dielectric elastomer films are insulated with rubberlike structures that are capable of undergoing reversible extension and producing work. Thus, an elastomer film needs to be capable of sustaining a large area expansion strain without suffering any damage and losing electric charging on the electrodes.<sup>15</sup>

Various dielectric elastomers, such as acryl rubbers,<sup>16–20</sup> thermoplastic elastomers,<sup>21–23</sup> and silicone elastomers,<sup>24–31</sup> have already



**Scheme 1.** Illustration of the setup for the actuation strain measurements. [Color figure can be viewed in the online issue, which is available at [wileyonlinelibrary.com](http://wileyonlinelibrary.com).]

been investigated as DEAs. The elastomer VHB 4905 from 3M was reported to provide excellent performance for highly prestrained films, but the handling of this product is quite difficult because of its sticky nature. The poly[styrene-*b*-(ethylene-*co*-butylene)-*b*-styrene] block polymer thermoplastic elastomer containing aliphatic mineral oil was a good system for understanding the actuation mechanism of DEAs with large actuation strains but showed fatal disadvantages, such as the leakage of mineral oil.<sup>32–34</sup>

Silicone elastomers have desirable properties, including a high energy efficiency, fast response, and good durability, because of their low viscoelastic losses, good resilience, and low electrical leakage. Silicone elastomers also have good temperature and humidity tolerance. Several commercial silicone elastomers have already been investigated as promising DEA products.<sup>29</sup> However, commercial silicone elastomers, such as Sylgard 184A, need further improvement in their mechanical and actuation properties because of some disadvantages, including their high modulus, small actuation strain, and weak tearing strength.<sup>35</sup>

In this work, our aim was to develop a straightforward and industrially scalable silicone elastomer actuator not only with improved mechanical properties (e.g., low modulus, high tearing strength, good resilience) but also with improved electromechanical actuation properties. Silicone elastomers were fabricated via a hydrosilylation addition reaction with vinyl-end-functionalized poly(dimethyl siloxane)s (Vs), a multivinyl-functionalized silicone resin (R), and a crosslinker in the presence of a platinum catalyst at an elevated temperature. The effects of the molecular weight of poly(dimethyl siloxane) (PDMS) and the resin and hardener contents on the tensile, dielectric, and electromechanical properties of the silicone elastomers were investigated to determine the optimum composition of the silicone DEA.

## EXPERIMENTAL

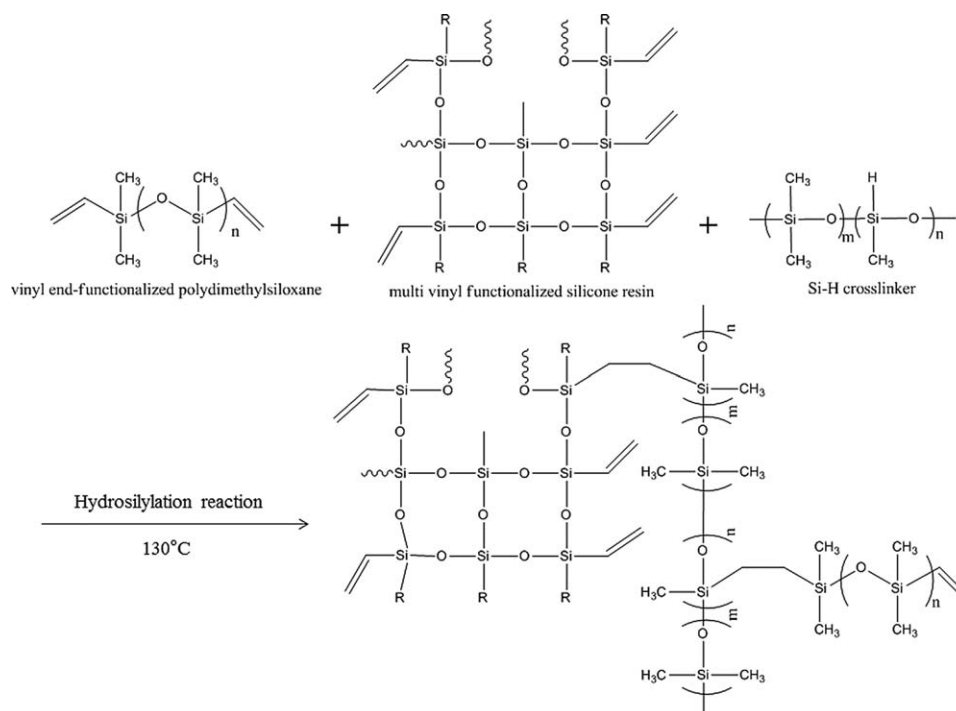
### Materials

The V, R, Si—H functionalized hardener (H), retarder, and Pt catalyst were supplied by KCC Corp. (Republic of Korea).

The chemical structures of V, R, and H are illustrated in Scheme 2. The five V samples had various vinyl molar contents, viscosities, and molecular weights, as listed in Table I. The viscosities of the V samples were 0.45, 1, 10, 70, and 150 kCP. The vinyl content of R was 0.7 mmol/g. The Si—H content of H was 2.3 mmol/g. Vinyl methyl cyclosiloxane was used as the retarder. A commercial silicone elastomer (Sylgard 184A) was purchased from Dow Corning. Xylene solvent was purchased from Daejung Chemicals (Republic of Korea).

### Fabrication of the Silicone Elastomer Films via Hydrosilylation

The silicone dielectric elastomer films were fabricated via a hydrosilylation reaction, as illustrated in Scheme 2. The vinyl groups in V and R and the Si—H groups of H were reacted to form  $\text{CH}_2\text{CH}_2\text{—Si}$  covalent bonds via a Pt-catalyzed hydrosilylation reaction at an elevated temperature. The vinyl methyl cyclosiloxane retarder prevented a hydrosilylation reaction during premixing at low temperature and allowed the reaction to proceed only at an elevated temperature. For the fabrication of the silicone dielectric elastomer films, initially V, R, the retarder, and the Pt catalyst were mixed together in xylene at different mass ratios according to the compositions presented in Table II. The concentrations of the Pt catalyst and the vinyl methyl cyclosiloxane retarder were fixed at 60 ppm and 0.067 mg, respectively, in the mixtures. Then, H was added to the mixture and mixed homogeneously. The xylene solvent and entrapped bubbles were removed *in vacuo*. The resulting resinous mixture was coated on the polyimide film to form silicone elastomer films with a thickness of 150  $\mu\text{m}$  with a bar coating device. The curing was carried out at elevated temperature at approximately 135°C for 4 h *in vacuo*. In a typical sample with a notation such as  $V_{150}H_{1.5}R_{10}$ ,  $V_{150}$  indicates a V with a viscosity of 150 kCP,  $H_{1.5}$  indicates that the relative molar ratio of the Si—H functional groups of H to the vinyl groups of V was 1.5, and  $R_{10}$  represents a resin content of 10 wt % in the silicone elastomer.



**Scheme 2.** Illustration of the hydrosilylation reaction.

### Characterization

The molecular weight and molecular weight distribution were determined with gel permeation chromatography (TS Science-Jasco) with toluene as the solvent. The  $^1\text{H-NMR}$  and  $^{13}\text{C-NMR}$  spectra were recorded on a Bruker 400-MHz high-resolution Fourier transform NMR spectrophotometer with  $\text{CDCl}_3$  as the solvent. The film thickness was measured with a micrometer (Heidenhain, MT2501). The dielectric constant ( $K$ ) and dielectric loss tangent ( $\tan \delta$ ) of the sample films were measured with an impedance analyzer (HP4192A) with a dielectric test fixture (Agilent 16089A) at 100 kHz at room temperature. The tensile properties were measured at an extension rate of 10 mm/min at room temperature with a universal testing machine (H5KT) with the ASTM D 882 standard method. The sample dimensions for the mechanical tests were  $50 \times 10 \text{ mm}^2$  (Length  $\times$  Width). The cyclic load-unload tensile test was implemented at an extension and contraction rate of 20 mm/min. The electromechanical transverse actuation strain

( $S_t$ ) was measured with a laser displacement sensor (Keyence LK-G80), as illustrated in Scheme 1. The polymer film had one end clamped at a fixed solid base and the other end was fixed with a cantilever at a different solid base. The polymer film was under slight tension because of the cantilever holding the film. When the voltage was applied to the film, its electromechanical deformation caused the end of the flexible cantilever to move back and forth. A laser displacement sensor measured the distance between the cantilever and the laser sensor. The usual dimensions of the films for actuation were  $25 \times 35 \text{ mm}^2$ . Carbon grease electrodes with dimensions of  $15 \times 25 \text{ mm}^2$  were coated on both surfaces of the film. The strain measurements were measured under a 0.2-Hz alternating-current (ac) electric signal. The electric voltage was delivered to the film with a function generator (Agilent 33250A) and amplified by a factor of 1000 through a high-voltage lock in an amplifier.  $S_t$  was defined as the change in length ( $\Delta L$ ) of the sample divided by the initial length ( $L_0$ ):

**Table I.** Characterizations of the Materials

	Viscosity (kcP)	$M_n$ (g/mol)	$M_w$ (g/mol)	$M_w/M_n$	O-CH=CH <sub>2</sub> (mmol/g)	Si-H (mmol/g)
R					0.7	
V <sub>0.5</sub>	0.45	11,376	24,571	2.16	0.17	
V <sub>1</sub>	1	16,426	33,788	2.06	0.12	
V <sub>10</sub>	10	39,799	75,954	1.91	0.053	
V <sub>70</sub>	70	53,082	100,322	1.89	0.027	
V <sub>150</sub>	150	85,320	158,859	1.86	0.021	
H						2.3

$M_n$  = number-average molecular weight;  $M_w$  = weight-average molecular weight.

**Table II.** Compositions of Silicone Dielectric Elastomers

Sample	V (g)					R (g)	Retarder (mg)	Pt (ppm)	H (g)
	V <sub>0.5</sub>	V <sub>1</sub>	V <sub>10</sub>	V <sub>70</sub>	V <sub>150</sub>				
V <sub>0.5</sub> H <sub>1.5</sub> R <sub>0</sub>	30					0	0.067	60	3.41
V <sub>1</sub> H <sub>1.5</sub> R <sub>0</sub>		30				0	0.067	60	2.35
V <sub>10</sub> H <sub>1.5</sub> R <sub>0</sub>			30			0	0.067	60	1.04
V <sub>70</sub> H <sub>1.5</sub> R <sub>0</sub>				30		0	0.067	60	0.53
V <sub>150</sub> H <sub>1.5</sub> R <sub>0</sub>					30	0	0.067	60	0.42
V <sub>150</sub> H <sub>1.5</sub> R <sub>5</sub>					30	1.5	0.067	60	1.11
V <sub>150</sub> H <sub>1.5</sub> R <sub>10</sub>					30	3	0.067	60	1.79
V <sub>150</sub> H <sub>1.5</sub> R <sub>15</sub>					30	4.5	0.067	60	2.48
V <sub>150</sub> H <sub>1.5</sub> R <sub>20</sub>					30	6	0.067	60	3.16
V <sub>150</sub> H <sub>1.5</sub> R <sub>25</sub>					30	7.5	0.067	60	3.85
V <sub>10</sub> H <sub>1.5</sub> R <sub>5</sub>			30			1.5	0.067	60	1.73
V <sub>70</sub> H <sub>1.5</sub> R <sub>5</sub>				30		1.5	0.067	60	1.21
V <sub>150</sub> H <sub>1.5</sub> R <sub>5</sub>					30	1.5	0.067	60	1.11
V <sub>10</sub> H <sub>3.0</sub> R <sub>5</sub>			30			1.5	0.067	60	3.44
V <sub>70</sub> H <sub>3.0</sub> R <sub>5</sub>				30		1.5	0.067	60	2.42
V <sub>150</sub> H <sub>3.0</sub> R <sub>5</sub>					30	1.5	0.067	60	2.19
V <sub>10</sub> H <sub>4.5</sub> R <sub>5</sub>			30			1.5	0.067	60	5.17
V <sub>70</sub> H <sub>4.5</sub> R <sub>5</sub>				30		1.5	0.067	60	3.64
V <sub>150</sub> H <sub>4.5</sub> R <sub>5</sub>					30	1.5	0.067	60	3.29

$$S_t(\%) = \frac{\Delta L}{L_0} \times 100 \quad (2)$$

## RESULTS AND DISCUSSION

This research was focused to develop a useful silicone elastomer actuator with enhanced mechanical properties (low modulus, high tearing strength, and good resilience) and electromechanical actuation properties. Figure 1 shows the <sup>1</sup>H-NMR spectra of representative V, H, and R. As Figure 1(a) shows that V<sub>150</sub> had two sets of characteristic peaks around 0.2 and 6 ppm. The peaks between 0.1 and 0.4 ppm represented the methyl groups attached to the silicone atoms and indicated that the main backbone structure was PDMS. The other peaks between 5.7 and 6.3 ppm indicated the presence of vinyl groups at the end of PDMS. As shown in Figure 1(b), H also had two sets of characteristic peaks around 0.2 and 4.7 ppm. The peaks at 0.2 ppm represented the methyl groups attached to the silicone atoms, whereas the peak at 4.7 ppm indicated the presence of Si—H functional groups. As shown in Figure 1(c), the resin (R) revealed three sets of characteristic peaks around 0.2, 1.3, and 6 ppm. The peaks between 0.1 and 0.3 ppm represented the methyl groups attached to the silicone atoms. The other peaks between 1.2 and 1.4 ppm indicated the hydroxyl groups attached to the silicone atoms. The peaks between 5.7 and 6.3 ppm revealed the presence of vinyl groups attached to the silicone atoms. The detailed peak assignments are presented in Figure 1. From the <sup>1</sup>H-NMR and gel permeation chromatography results, the molar concentrations of the vinyl and Si—H functional groups in V, R, and H were calculated, as listed in Table I.

Figure 2 shows the stress–strain curves and the resulting tensile modulus (*E*) and elongation at break ( $\epsilon_b$ ) of the silicone elastomers with various weight-average molecular weights of V. The relative molar ratio of Si—H groups in H to the vinyl groups in V was fixed at 1.5. The silicone elastomers were free of R. The detailed mechanical properties are listed in Table II. The sample V<sub>0.5</sub>H<sub>1.5</sub>R<sub>0</sub>, with a molecular weight of V of 0.45 kg/mol, revealed an *E* of 0.99 MPa and an  $\epsilon_b$  of 57%. As the molecular weight of V increased,  $\epsilon_b$  increased; in contrast, *E* decreased. The sample V<sub>150</sub>H<sub>1.5</sub>R<sub>0</sub>, with a molecular weight of V of 150 kg/mol, had an *E* value of 0.20 MPa and an  $\epsilon_b$  of 262%.

Figure 3 shows the *E* and  $\epsilon_b$  of silicone elastomers with various R contents. The relative molar ratio of Si—H to vinyl in the silicone elastomer was fixed at 1.5. The value of *E* increased linearly with increasing R content. However,  $\epsilon_b$  increased with increasing R content up to 10 wt % and then decreased with further increases in the R content. The resin-free V<sub>150</sub>H<sub>1.5</sub>R<sub>0</sub> had an  $\epsilon_b$  of 262%. V<sub>150</sub>H<sub>1.5</sub>R<sub>10</sub>, with an R content of 10%, had the largest  $\epsilon_b$  of 311%, whereas V<sub>150</sub>H<sub>1.5</sub>R<sub>25</sub>, with an R content of 25%, had the smallest  $\epsilon_b$  of 125%. That is, the incorporation of small amounts of R into the silicone elastomer improved the tearing strain and strength.

Figure 4 shows the variation of *E* and  $\epsilon_b$  of the silicone elastomers with H contents. The R content was fixed at 5 wt %. As H content increased, *E* increased slightly, whereas  $\epsilon_b$  decreased. The effect of the hardener was stronger in the low V molecular weight rather than in the high V molecular weight. V<sub>10</sub> showed a larger increase than V<sub>150</sub> in *E* as the H content increased.

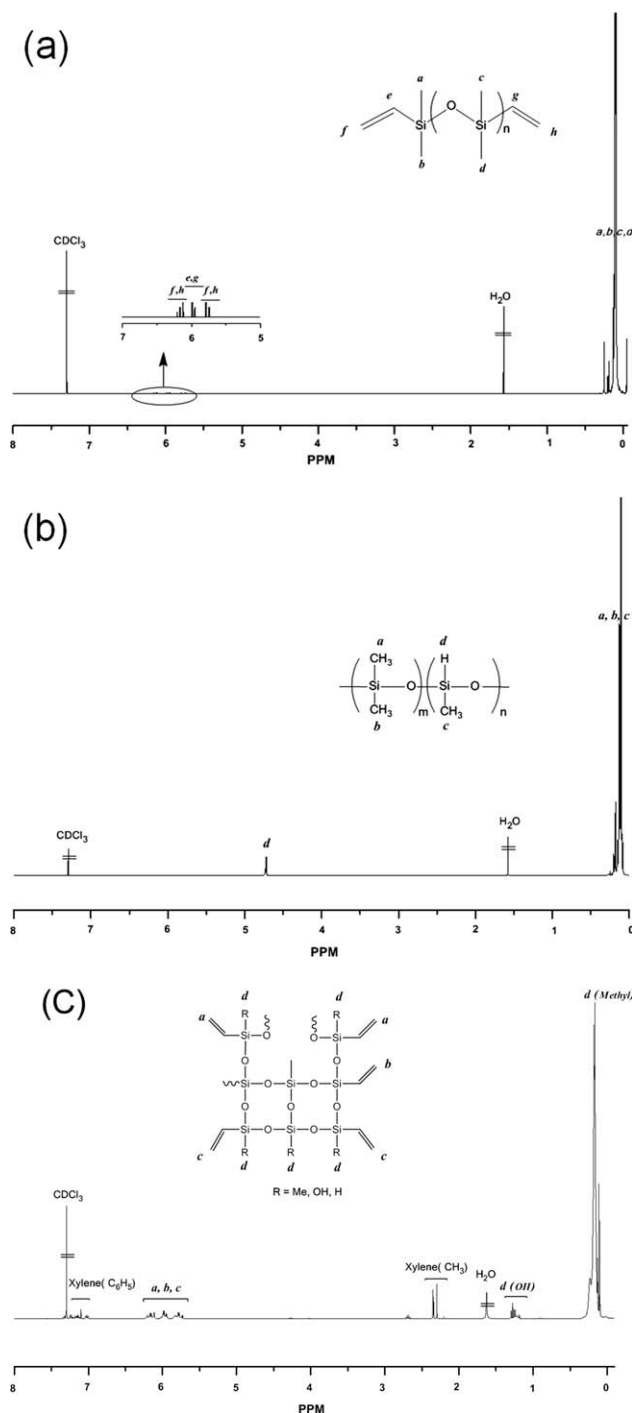


Figure 1.  $^1\text{H-NMR}$  spectra of (a) V, (b) H, and (c) R.

Figure 5(a) shows representative cyclic load–unload examination graphs of the  $\text{V}_{150}\text{H}_{1.5}\text{R}_0$  silicone elastomers. For a better display, each cyclic curve was vertically shifted on the  $y$  axis. Each specimen was examined in a four-cycle load–unload test to evaluate the resilience properties. The maximum extension in the examinations was 150%. In the first load–unload cycle, the  $\text{V}_{150}\text{H}_{1.5}\text{R}_0$  sample showed a small hysteresis. The hysteresis resulted in a permanent residual strain that remained even after the load was completely removed. In the second to

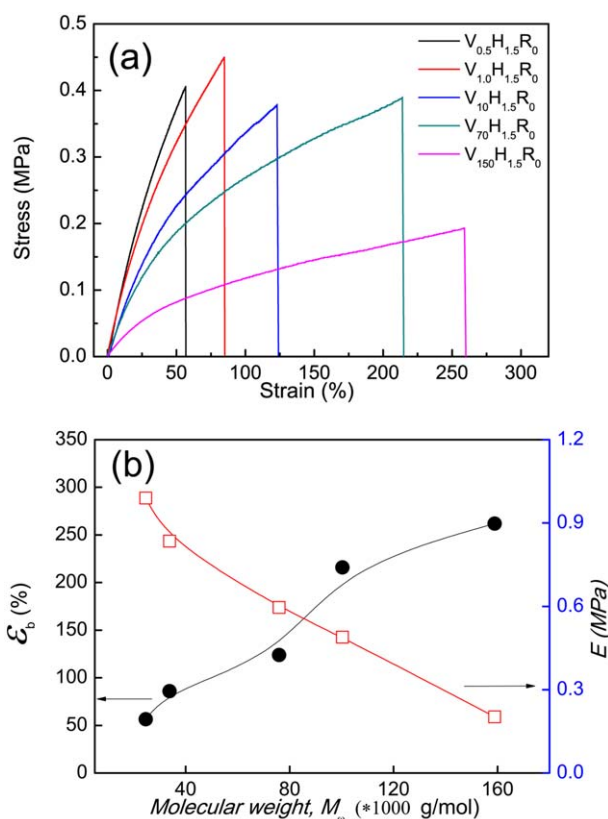
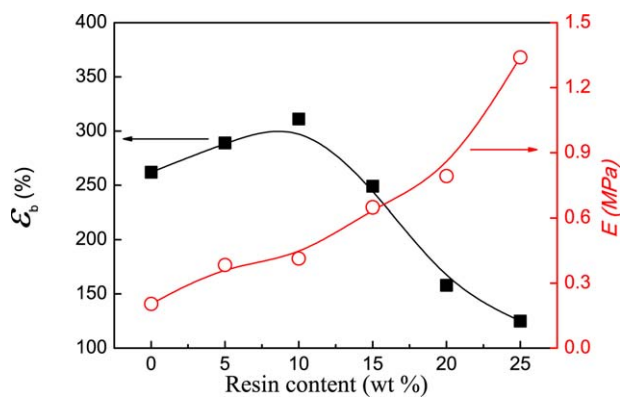


Figure 2. (a) Stress–strain curves and (b) the resulting  $E$  and  $\varepsilon_b$  values of silicone elastomers with different molecular weights. [Color figure can be viewed in the online issue, which is available at wileyonlinelibrary.com.]

fourth cycles, the  $\text{V}_{150}\text{H}_{1.5}\text{R}_0$  sample hardly revealed further hysteresis behavior; this indicated the development of no further residual strain during these cycles. Figure 5(b) shows the first cycles in the load–unload examination of the silicone elastomers at various molecular weights of V. Each curve was vertically shifted for a better display. The  $\text{V}_{0.5}\text{H}_{1.5}\text{R}_0$ ,  $\text{V}_1\text{H}_{1.5}\text{R}_0$ , and  $\text{V}_{10}\text{H}_{1.5}\text{R}_0$  samples were ruptured before 150% extension. Samples with a larger molecular weight provided larger  $\varepsilon_b$ 's. The  $\text{V}_{70}\text{H}_{1.5}\text{R}_0$  and  $\text{V}_{150}\text{H}_{1.5}\text{R}_0$  samples revealed residual strains of 4.8 and 4.5%, respectively. These results indicate that the stretchability and resilience of the silicone elastomers improved with increasing molecular weight of V. We observed that the residual strains also depended on the R and H contents. Figure 5(c) shows the residual strain of  $\text{V}_{150}\text{H}_{1.5}$  with various R contents. Sample  $\text{V}_{150}\text{H}_{1.5}\text{R}_0$  (without R) provided a residual strain of 4.5%. In the presence of R, the  $\text{V}_{150}\text{H}_{1.5}\text{R}_5$ ,  $\text{V}_{150}\text{H}_{1.5}\text{R}_{10}$ ,  $\text{V}_{150}\text{H}_{1.5}\text{R}_{15}$ , and  $\text{V}_{150}\text{H}_{1.5}\text{R}_{20}$  samples revealed the same residual strain of 7.2%. Figure 5(d) shows the residual strains of  $\text{V}_{150}\text{R}_0$  with various H contents. The residual strain monotonously increased with increasing H content.

The measured  $K$  values and  $\tan \delta$  values of the silicone elastomers at a frequency of 100 kHz are listed in Table III. The dielectric properties of the silicone elastomers hardly depended on the molecular weight of V or on the R and H contents. Regardless of the sample composition, the silicone





**Figure 3.**  $E$  and  $\epsilon_b$  values of silicone elastomers with various R contents. [Color figure can be viewed in the online issue, which is available at [wileyonlinelibrary.com](http://wileyonlinelibrary.com).]

elastomer provided almost the same  $K_s$  of 3.26–3.34 and  $\tan \delta$  values of 0.0003–0.003 at 7–100 kHz. The dielectric properties are determined by the chemical structures of the polymers, and all of the silicone polymers in this study revealed almost the same chemical structures.<sup>36</sup> The  $\tan \delta$ , which results from the inelastic rotation of the dipoles in the sample under an electric field, is related to the internal energy dissipation and energy consumption during electromechanical

actuation.<sup>14–16</sup> Thus, the produced silicone elastomers were capable of being used as an energy-efficient polymer actuators with a small energy loss.

Figure 6(a) shows the  $S_t$  values of the  $V_{150}H_{1.5}R_0$  silicone elastomer at various ac electric field strengths.  $S_t$  was calculated with eq. (2) on the basis of the peak-to-peak strain at each electric field. The  $S_t$  value increased with increasing applied electric field. Figure 6(b) shows the variation of  $S_t$  of silicone elastomers with various molecular weights of V. The commercial Sylgard 184A silicone elastomer was compared with these as a reference. In every sample, the  $S_t$  value was proportional to the square of the applied electric field. The actuation strain curves agreed with the characteristic electric actuation behavior of the electrostrictive DEA.<sup>1</sup> The actuation strains strongly depended on the molecular weight of the polymer. The  $S_t$  value increased with increasing molecular weight of V. All of the silicone elastomers in this study provided larger actuation strains than the commercial silicone 184A. Sample  $V_{150}H_{1.5}R_0$  revealed an  $S_t$  value of 0.82% at  $50 \text{ V}/\mu\text{m}$ , which was four times larger than that of 184A. Figure 6(c) shows the  $S_t$  variation of the silicone elastomer samples with various R contents. The  $S_t$  value decreased with increasing R content at the same electric field strength. Figure 6(d) shows the  $S_t$  variation of the silicone elastomer samples with various H contents. The  $S_t$  value decreased with increasing H content at the same electric field strength.

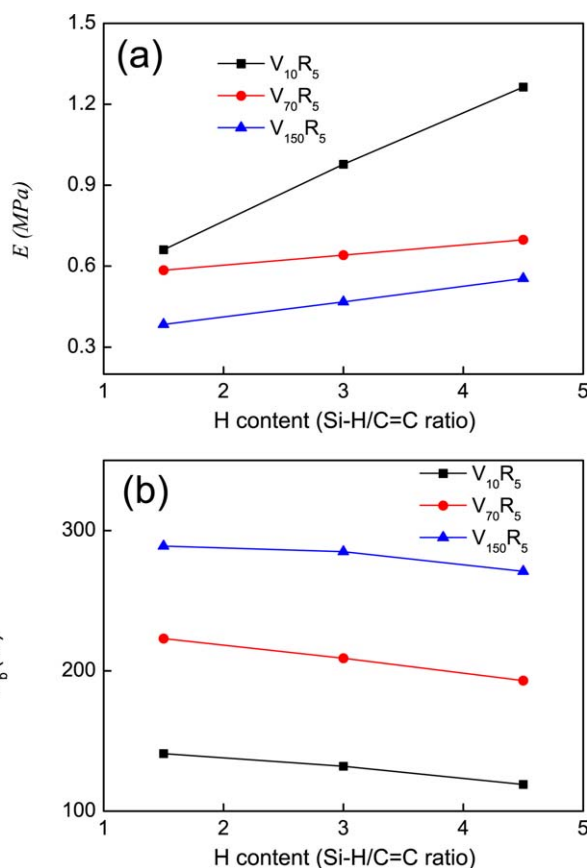


**Figure 4.** (a)  $E$  versus H content and (b)  $\epsilon_b$  versus H content of the silicone elastomers. [Color figure can be viewed in the online issue, which is available at [wileyonlinelibrary.com](http://wileyonlinelibrary.com).]

In this study, the effects of the molecular weight of V and the amounts of R and H on the mechanical, dielectric, and electromechanical properties of the silicone elastomers were investigated. The dielectric properties, such as  $K$  and  $\tan \delta$ , of the silicone elastomers were observed to be independent of the molecular weight of V and the amounts of R and H because the chemical features of the silicone elastomers were the same. However, the mechanical and electromechanical properties of the silicone elastomers were significantly affected by the molecular weight of V and the R and H contents.

With regard to the mechanical properties, as the molecular weight of V increased, the  $E$  values of the silicone elastomers decreased, but the  $\epsilon_b$  and resilience values increased. In contrast, when the H content increased,  $E$  and the residual strain of the silicone elastomers increased, and  $\epsilon_b$  decreased. Basically, the modulus of the elastomers with a network structure depended on the crosslinking density, which was a function of the chain length between the crosslinking points, as shown in eq. (3).<sup>37</sup>

$$E = \rho R_{\text{air}} T / M_c \quad (3)$$

where  $\rho$ ,  $R_{\text{air}}$ ,  $T$ , and  $M_c$  represent the density, ideal gas constant, temperature, and molecular weight between crosslinking points, respectively. As the  $M_c$  value between the crosslinking points increased, the crosslinking density decreased, and the modulus decreased. With the assumption that all of the vinyl groups of V participated in the hydrosilylation crosslinking reaction, the molecular weight of V would be equivalent to  $M_c$ . As a result, when the molecular weight of V increased, the  $E$  values of the silicone elastomers decreased, according to eq. (3). The softer elastomer with a large  $M_c$  value provided a larger  $\epsilon_b$  and a smaller hysteresis in the cyclic test. Because of the same

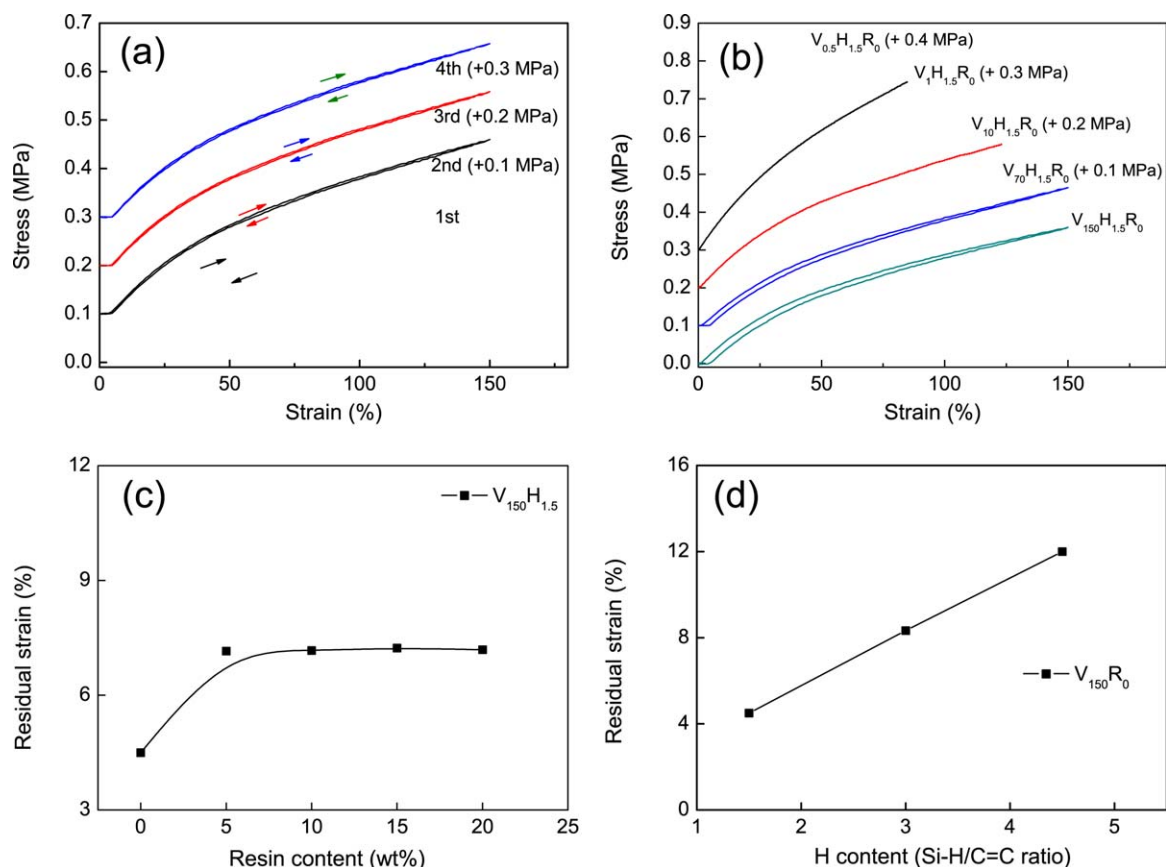


**Figure 5.** (a) Cyclic load–unload examination of  $V_{150}H_{1.5}R_0$  silicone elastomers during four cycles. For a better display, each cyclic curve was vertically shifted on the  $y$  axis. (b) First cycle load–unload examination of the silicone elastomers at various molecular weights of  $V$ . (c) Residual strain of  $V_{150}H_{1.5}$  with various  $R$  contents. (d) Residual strain of  $V_{150}R_0$  with various  $H$  contents. [Color figure can be viewed in the online issue, which is available at [wileyonlinelibrary.com](http://wileyonlinelibrary.com).]

reason, when the  $H$  content increased, the crosslinking density and  $E$  values of the silicone elastomers increased. The stiffer elastomer with a large  $H$  content provided a smaller  $\varepsilon_b$  value and a larger hysteresis in the cyclic test.

Interestingly, when the  $R$  content increased, the  $E$  values of the silicone elastomers monotonously increased; however, the  $\varepsilon_b$  value increased up to 10 wt % and then decreased. This modulus behavior was explained by the fact that the  $R$  played a role

**Table III.** Mechanical, Dielectric, and Actuation Properties of the Silicone Dielectric Elastomers with Various Compositions

Sample	$E$ (MPa)	$\varepsilon_b$ (%)	$K$ at 100 kHz	$\tan \delta$ at 100 MHz	$S_t$ at 50 V/ $\mu\text{m}$ (%)
184A	0.24	93	3.33	0.0007	0.19
$V_{0.5}H_{1.5}R_0$	0.99	57	3.26	0.0001	0.28
$V_{1}H_{1.5}R_0$	0.84	86	3.25	0.0007	0.33
$V_{10}H_{1.5}R_0$	0.6	124	3.31	0.0008	0.43
$V_{70}H_{1.5}R_0$	0.49	216	3.26	0.001	0.62
$V_{150}H_{1.5}R_0$	0.2	262	3.33	0.0003	0.83
$V_{150}H_{1.5}R_5$	0.38	289	3.38	0.0013	0.71
$V_{150}H_{1.5}R_{10}$	0.41	311	3.33	0.0014	0.59
$V_{150}H_{1.5}R_{15}$	0.65	249	3.3	0.0007	0.43
$V_{150}H_{1.5}R_{20}$	0.79	158	3.34	0.002	0.27
$V_{150}H_{1.5}R_{25}$	1.34	125	3.33	0.001	0.25
$V_{70}H_{1.5}R_5$	0.59	223	3.3	0.0021	0.51
$V_{70}H_{3.0}R_5$	0.64	209	3.22	0.0022	0.38
$V_{70}H_{4.5}R_5$	0.7	193	3.27	0.003	0.26

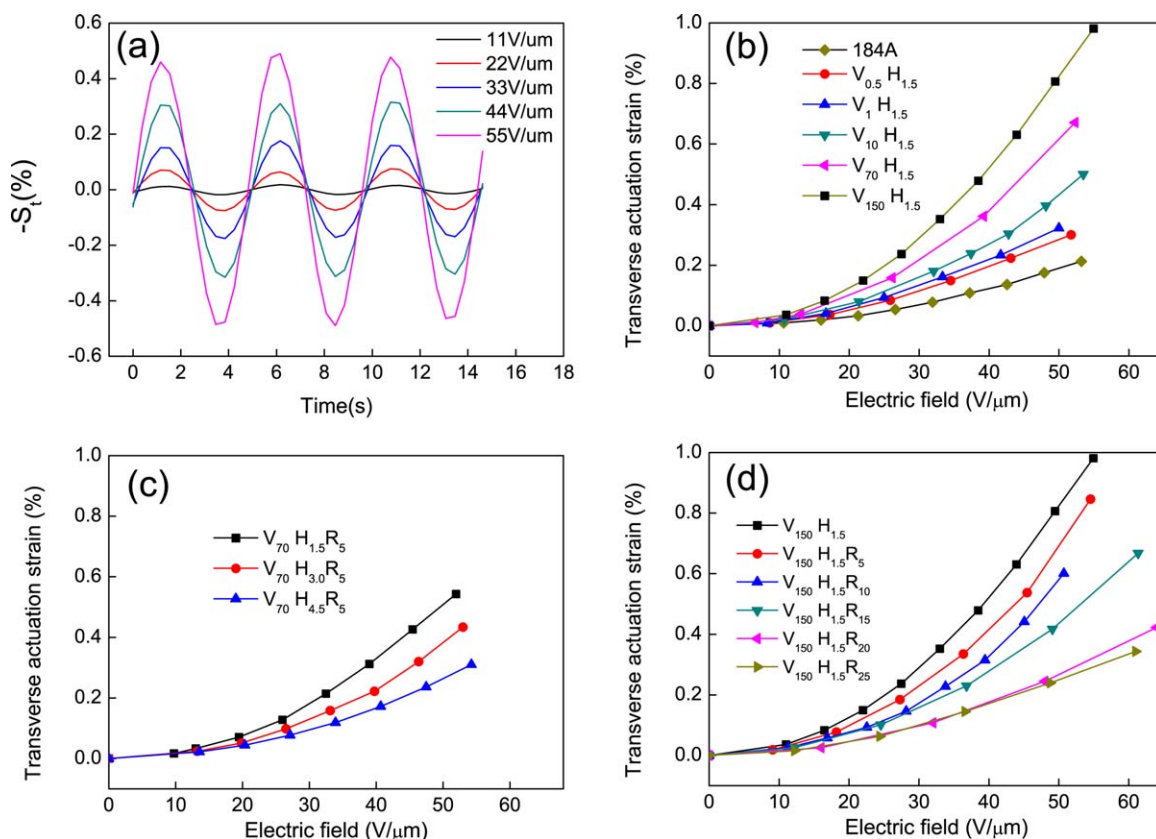


**Figure 6.** (a)  $S_t$  of the  $V_{150}H_{1.5}R_0$  silicone elastomer at various ac electric field strengths. (b)  $S_t$  of silicone elastomers with various molecular weights of V, (c)  $S_t$  of silicone elastomers with various R contents, and (d)  $S_t$  of silicone elastomers with various H contents. [Color figure can be viewed in the online issue, which is available at [wileyonlinelibrary.com](http://wileyonlinelibrary.com).]

as a crosslinking point like the hardener. At small amounts of R, the increase in the crosslinking density of the silicone elastomer improved both the tearing strain and strength because the resins acted as strong crosslink points. However, a high concentration of R caused a reduction in the tearing strain of the elastomer because of the large increase in the stiffness. That is, the addition of a small amount of R increased the crosslinking density and the tearing strength.

The electromechanical properties of the silicone elastomers depended significantly on the molecular weight of V and the R and H contents. As the molecular weight of V increased,  $S_t$  increased. In contrast, when the R and H contents increased,  $S_t$  decreased. This actuation behavior may have been due to electromechanical responses that were observed to be reciprocal to the moduli of the elastomers, as shown in eq. (1). The modulus decreased with increasing molecular weight of V and decreased with increasing amounts of H and R in the products.

## CONCLUSIONS

Silicone elastomers were fabricated via a hydrosilylation addition reaction with V, R, and a Si—H functionalized crosslinker. The mechanical and electromechanical properties of the silicone elastomers were observed to be easily controllable with the molecular weight of PDMS, the resin content, and the hardener content. To get a larger  $s$ , a larger molecular weight of PDMS, a

lower hardener content, and a resin-free composition should be used. However, the silicone DEA needed to include a small amount of resin to improve the tearing strength.

## ACKNOWLEDGMENTS

This work was financially supported by a grant from the Fundamental R&D Program for Core Technology of Materials, which is funded by the Ministry of Knowledge Economy of the Republic of Korea, and partially by a grant from the Center for Materials Architecturing of the Korea Institute of Science and Technology.

## REFERENCES

- Pelrine, R. E.; Kornbluh, R. D.; Joseph, J. P. *Sens. Actuators A* **1998**, *64*, 77.
- Pelrine, R.; Kornbluh, R.; Pei, Q. B.; Joseph, J. *Science* **2000**, *287*, 836.
- Zhang, Q. M.; Li, H. F.; Poh, M.; Xia, F.; Cheng, Z. Y.; Xu, H. S.; Huang, C. *Nature* **2002**, *419*, 284.
- Shankar, R.; Ghosh, T. K.; Spontak, R. *J. Soft Matter* **2007**, *3*, 1116.
- Koo, I. M.; Jung, K.; Koo, J. C.; Nam, J. D.; Lee, Y. K.; Choi, H. R. *IEEE Trans. Robotics* **2008**, *24*, 549.
- Anderson, I. A.; Gisby, T. A.; McKay, T. G.; O'Brien, B. M.; Calius, E. P. *J. Appl. Phys.* **2012**, *112*.



7. Carpi, F.; Bauer, S.; De Rossi, D. *Science* **2010**, *330*, 1759.
8. Carpi, F.; Frediani, G.; Turco, S.; De Rossi, D. *Adv. Funct. Mater.* **2011**, *21*, 4152.
9. Kwak, J. W.; Chi, H. J.; Jung, K. M.; Koo, J. C.; Jeon, J. W.; Lee, Y.; Nam, J. D.; Ryew, Y.; Choi, H. R. *J. Mech. Sci. Technol.* **2005**, *19*, 578.
10. Aschwanden, M.; Beck, M.; Stemmer, A. *IEEE Photonics Technol. Lett.* **2007**, *19*, 1090.
11. Doll, A. F.; Wischke, M.; Geipel, A.; Goldschmidtboeing, F.; Ruthmann, O.; Hopt, U. T.; Schrag, H. J.; Woias, P. *Sens. Actuators A* **2007**, *139*, 203.
12. Brochu, P.; Pei, Q. B. *Macromol. Rapid Commun.* **2010**, *31*, 10.
13. Niu, X. F.; Yang, X. G.; Brochu, P.; Stoyanov, H.; Yun, S.; Yu, Z. B.; Pei, Q. B. *Adv. Mater.* **2012**, *24*, 6513.
14. Zhang, Q. M.; Su, J.; Kim, C. H.; Ting, R.; Capps, R. J. *Appl. Phys.* **1997**, *81*, 2770.
15. Pelrine, R.; Sommer-Larsen, P.; Kornbluh, R.; Heydt, R.; Kofod, G.; Pei, Q. B.; Gravesen, P. *Smart Struct. Mater.* **2001**, 4329, 335.
16. Kofod, G.; Sommer-Larsen, P.; Kronbluh, R.; Pelrine, R. J. *Intell. Mater. Syst. Struct.* **2003**, *14*, 787.
17. Wissler, M.; Mazza, E. *Sens. Actuators A* **2007**, *134*, 494.
18. Jordi, C.; Michel, S.; Kovacs, G.; Ermanni, P. *Sens. Actuators A* **2010**, *161*, 182.
19. Keplinger, C.; Kaltenbrunner, M.; Arnold, N.; Bauer, S. *Proc. Natl. Acad. Sci. U.S.A.* **2010**, *107*, 4505.
20. Huang, J. S.; Shian, S.; Diebold, R. M.; Suo, Z. G.; Clarke, D. R. *Appl. Phys. Lett.* **2012**, *101*, 122905.
21. Shankar, R.; Ghosh, T. K.; Spontak, R. J. *Adv. Mater.* **2007**, *19*, 2218.
22. Shankar, R.; Krishnan, A. K.; Ghosh, T. K.; Spontak, R. J. *Macromolecules* **2008**, *41*, 6100.
23. Vargantwar, P. H.; Ozcam, A. E.; Ghosh, T. K.; Spontak, R. J. *Adv. Funct. Mater.* **2012**, *22*, 2100.
24. Kussmaul, B.; Risse, S.; Kofod, G.; Wache, R.; Wegener, M.; McCarthy, D. N.; Kruger, H.; Gerhard, R. *Adv. Funct. Mater.* **2011**, *21*, 4589.
25. Kofod, G.; Sommer-Larsen, P. *Sens. Actuators A* **2005**, *122*, 273.
26. Carpi, F.; Salaris, C.; De Rossi, D. *Smart Mater. Struct.* **2007**, *16*, S300.
27. Carpi, F.; Gallone, G.; Galantini, F.; De Rossi, D. *Adv. Funct. Mater.* **2008**, *18*, 235.
28. O'Halloran, A.; O'Malley, F.; McHugh, P. *J. Appl. Phys.* **2008**, *104*, 071101.
29. Michel, S.; Zhang, X. Q.; Wissler, M.; Lowe, C.; Kovacs, G. *Polym. Int.* **2010**, *59*, 391.
30. Opris, D. M.; Molberg, M.; Walder, C.; Ko, Y. S.; Fischer, B.; Nuesch, F. A. *Adv. Funct. Mater.* **2011**, *21*, 3531.
31. Zhao, H.; Wang, D. R.; Zha, J. W.; Zhao, J.; Dang, Z. M. *J. Mater. Chem. A* **2013**, *1*, 3140.
32. Kim, B.; Park, Y. D.; Min, K.; Lee, J. H.; Hwang, S. S.; Hong, S. M.; Kim, B. H.; Kim, S. O.; Koo, C. M. *Adv. Funct. Mater.* **2011**, *21*, 3242.
33. Kim, B.; Park, Y.; Kim, J.; Hong, S. M.; Koo, C. M. *J. Polym. Sci. Part B: Polym. Phys.* **2010**, *48*, 2392.
34. Kim, B.; Min, K.; Kim, J.; Hong, S. M.; Koo, C. M. *Mol. Cryst. Liq. Cryst.* **2010**, *519*, 77.
35. Khoo, M.; Liu, C. *Sens. Actuators A* **2001**, *89*, 259.
36. Tanaka, T. *IEEE Trans. Dielectr. Electr. Insul.* **2005**, *12*, 914.
37. Gedde, U. W. *Polymer Physics*; Kluwer Academic: Dordrecht, The Netherlands, **1995**.